Comptes Rendus

Chimie

Hammed Olawale Oloyede, Joseph Anthony Orighomisan Woods,
Helmar Görls, Winfried Plass and Abiodun Omokehinde Eseola

Influence of structural and thermal factors on phenoxazinone synthase activities catalysed by coordinatively saturated cobalt(III) octahedral complexes bearing diazene–disulfonamide NˆNˆN chelators

Full paper / *Mémoire*

Influence of structural and thermal factors on phenoxazinone synthase activities catalysed by coordinatively saturated cobalt(III) octahedral complexes bearing diazene–disulfonamide N^N^N chelators

Hammed Olawale Oloyede [a, b]**, Joseph Anthony Orighomisan Woods** [a]**, Helmar Görls** [b]**, Winfried Plass** [*, b] **and Abiodun Omokehinde Eseola** [●] [*, b, c]

[a] Inorganic Chemistry Unit, Department of Chemistry, University of Ibadan, Ibadan, Nigeria

[b] Institut für Anorganische und Analytische Chemie, Friedrich-Schiller-Universität Jena, Humboldtstraße 8, 07743 Jena, Germany

[c] Materials Chemistry group, Department of Chemical Sciences, Redeemer's University Ede, Osun State, Nigeria.

Current addresses: Institut für Anorganische und Analytische Chemie, Friedrich-Schiller-Universität Jena, Humboldtstr. 8, D-07743 Jena, Germany. (W. Plass), Institut für Anorganische und Analytische Chemie, Friedrich-Schiller-Universität Jena, Humboldtstr. 8, D-07743 Jena, Germany. (A. O. Eseola).

E-mails: sekr.plass@uni-jena.de (W. Plass), biodun.eseola@uni-jena.de (A. O. Eseola), bioduneseola@hotmail.com (A. O. Eseola).

Abstract. There are increasing efforts towards the development of new synthetic models that can mimic phenoxazinone synthase activity due to the important applications of several biomolecules bearing the phenoxazinone chromophore. However, deliberate studies of systematically varied coordination species for the knowledge of underlying molecular determinants of catalytic outcomes using fully characterized mimicking models are scarce. In this report, two new dianionic and synthetically obtained diazene–disulfonamide N^N^N chelators of the form $RSO_2–NH–Ph–N=N–Ph–NHSO_2R$ (R = methyl for **1** and tolyl for **2**) are coordinatively self-assembled around cobalt(III) centres in the presence or absence of co-ligands (acetate, bipyridine, 4-dimethylaminopyridine and/or water) to obtain four new and structurally analysed complexes [**Co1₂**][Et₃NH], **Co1**·OAc·bpy, **Co1**·OAc·bpy and **Co2**·dmap·w, which are all found to be octahedral cobalt(III) polyhedra, distorted to varying extents, by using Continuous Shape Measurement calculations. Based on structural and thermal factors, it is

* Corresponding authors.

observed that the trends of the phenoxazinone synthase mimicking activities by these complexes correlate with their inherent abilities to generate vacant coordination space for substrate–metal ion interactions. Finally, it is also observed that coordinative steric strains control catalytic trends among the complexes at low temperatures while susceptibility to thermal dissociations is the determinant at higher temperatures.

1. Introduction

The multi-copper metalloenzyme called phenoxazinone synthase is naturally found in *Streptomyces antibioticus* [1,2]. This metalloenzyme catalyses the oxidative coupling of 2-aminophenol (or o-aminophenol) derivatives [3–5], which leads to biomolecular building blocks of medicinally important anticancer and antibiotic macromolecules such as actinomycin-D, pitucamycin, dandamycin, chandrananimycin E, etc. (Scheme 1(a)) [6–9]. In biological systems, factors like substrate accessibility of the metal binding site, the presence of a secondary coordination sphere, ligand chelation characteristics, non-covalent interactions, hydrophobic/hydrophilic properties and hydrogen bonding have been recognized to influence the mimicking activity of metal complexes in different biochemical processes [10–13]. Therefore, we assumed that the design of a series of new cobalt(III) coordination materials in systematically varied coordination environments could improve the understanding of how specific coordination environments affect the enzyme mimicking behaviour of synthetic complexes. Such a structure–property correlation study holds the potential of enabling greater yields in the industrial preparation of the beneficial phenoxazinone chromophores.

Sulfonamide-based molecules have been known for several decades, and they occupy a significant place in biomolecular sciences [14–16] because of their importance in the development of numerous pharmaceuticals [17–20]. In organic synthesis, the use of sulfonamides as protecting groups and as excellent sources of introducing nitrogenous units into organic compounds is also well documented [21,22]. However, sulfonamide moieties are much less explored as N-donors in coordination chemistry. A few reports of complexes containing sulfonamide ligands are encountered for applications in magnetism [23,24], optics [25,26], catalysis [14,27,28] and drug design [29–32], but complexes of these biologically significant sulfonamide moieties are scarcely reported as functional models for mimicking metalloenzymes in biological systems [33] and so on.

We herein present the results of the syntheses, structural characterization and phenoxazinone synthase mimicking activity of octahedral cobalt(III) complexes bearing sterically varied tridentate diazene–disulfonamide N-donors, which are dianionic, as well as bidentate and monodentate N- and O-donor co-ligands (Scheme 1(b–c)).

2. Experimental section

2.1. *General information*

All starting materials for synthesis as well as substrates for the catalytic experiments were obtained commercially as reagent grades and used as supplied without further purification. The *o*-sulfonamide azobenzene ligands **1** and **2** have been previously prepared and reported [34]. IR spectra were measured with a Bruker Equinox FT-IR spectrometer equipped with a diamond ATR unit in the range of 4000–600 cm^{-1}. UV–Vis measurement was carried out using Varian Cary 5E UV-VIS-NIR Spectrophotometer. Elemental analyses were carried out on Leco CHNS-932 and El Vario III elemental analysers. Mass spectrometry (MS) spectra were measured with a Bruker MAT SSQ 710 spectrometer. ^{1}H and ^{13}C NMR spectra for characterization of the phenoxazinone product were recorded with a Bruker AVANCE 400 MHz spectrometer using deuterated solvents and TMS as the internal standard.

2.2. *Synthesis of cobalt(III) complexes*

Co1·OAc·bpy**:** Ligand **1** (51 mg, 0.14 mmol), 2,2-bipyridine (22 mg, 0.14 mmol) and cobalt(II) acetate
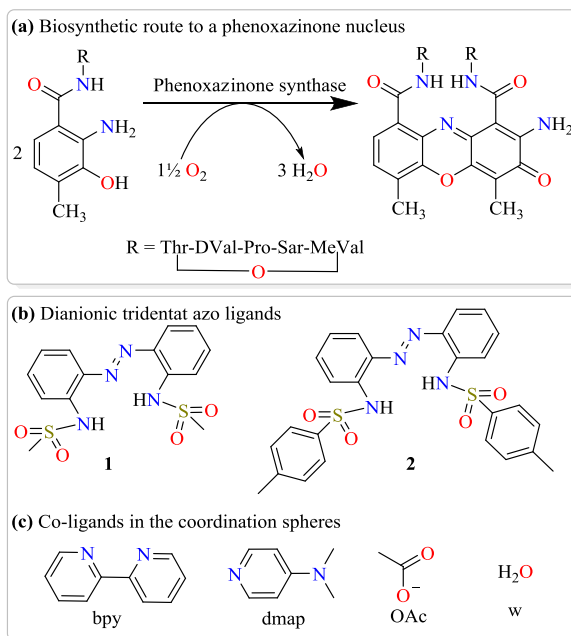
Scheme 1. (a) Biosynthesis of actinomycin-D catalysed by phenoxazinone synthase, (b) structures of synthesized chelating sulfonamides and (c) the co-ligands incorporated for cobalt(III) complex assembly in this study.

tetrahydrate (0.04 g, 0.14 mmol) reacted in 5 mL ethanol after which a 0.1 mL methanol solution of 0.05 M NaOH was added to the reaction mixture. The solution was kept under slow evaporation. After 2 weeks, **Co1**·OAc·bpy was obtained as purple crystals suitable for X-ray measurement. Yield (58 mg, 65%). M.p = 223 °C. Selected IR data (ATR, cm^{-1}): 3060w (Ar–H), 2965w (methyl), 1653m (C=O, acetate), 1606s (C=C, C=N), 1596vs (C=C, C=N), 1507m, 1445vs, 1243s, 1158m, 1119m, 1035m, 959s, 856s, 731s, 623m. MS (EI, Calc. m/z = 640.58): 502 (M – acetate – SO$_2$Me, 5%), 424 (M – bpy & OAc, 50%), 368 (ligand **1**), 345, 289, 267, 210, 156 (bpy, 100%), 128. Anal. calc. for C$_{24}$H$_{22}$CoN$_6$O$_4$S$_2$: C, 49.57; H, 3.81; N, 14.45; S, 11.03%. Found: C, 49.14; H, 3.83; N, 14.20; S, 10.84%.

[**Co1$_2$**][Et$_3$NH]**:** Ligand **1** (99 mg, 0.27 mmol) and cobalt(II) acetate tetrahydrate (35 mg, 0.14 mmol) reacted in methanol (2 mL) together with 0.1 mL of triethylamine (Et$_3$N). The solution was allowed to slowly evaporate for 2 weeks, which led to the formation of purple crystals that are suitable for X-ray measurement. Yield (61 mg, 25%). M.p = 301 °C. Selected IR data (ATR, cm^{-1}): 3073m (Ar–H), 2933w (methyl), 1595s (C=C, C=N), 1569s, 1474s, 1330s,

1300vs, 1244s, 1041s, 958vs, 867s, 840vs, 751s, 726vs, 625s. MS (ESI, Calc. m/z = 893.95): 916 (M + Na$^+$, 15%), 758 (M – 2 methyl – Et$_3$NH$^+$, 45%). Anal. calc. for C$_{34}$H$_{43}$CoN$_9$O$_8$S$_4$: C, 45.68; H, 4.96; N, 14.10; S, 14.35%. Found: C, 45.54; H, 4.98; N, 13.87; S, 14.13%.

Co2·OAc·bpy**:** Ligand **2** (53 mg, 0.10 mmol), 2,2-bipyridine (15 mg, 0.10 mmol) and cobalt(II)acetate tetrahydrate (26 mg, 0.10 mmol) were added together in 3 mL ethanol. 0.1 mL of 0.05 M methanol solution of NaOH was added to the reaction mixture. The solution was slowly evaporated. After 2 weeks, purple crystals of **Co2**·OAc·bpy suitable for X-ray measurement were obtained. Yield (63 mg, 79%). M.p = 236 °C. Selected IR data (ATR, cm^{-1}): 3063w (Ar–H), 2978w (methyl), 1606s (C=C, C=N), 1594s (C=C, C=N), 1569m, 1497s, 1451vs, 1357vs, 1295vs, 1247vs, 1159m, 1138vs, 1080vs, 965s, 911s, 836vs, 763vs, 686vs, 624vs. MS (ESI, Calc. m/z + Na$^+$ = 815.76): 815 (M + Na, 45%), 733 (M – acetate, 100%), 659 (M – bpy, 25%), 578 (ligand **2** + Co^{3+}, 20%). Anal. calc. for C$_{36}$H$_{30}$CoN$_6$O$_4$S$_2$·2H$_2$O: C, 55.07; H, 4.50; N, 10.14; S, 7.74%. Found: C, 54.99; H, 4.37; N, 10.11; S, 7.74%.

Co2·dmap·w**:** Ligand **2** (53 mg, 0.10 mmol), 4-dimethylaminopyridine (dmap) (12 mg, 0.10 mmol)

and cobalt(II)acetate tetrahydrate (26 mg, 0.10 mmol) reacted in ethanol (3 mL). The solution was slowly evaporated. After a week, yellowish crystals of **Co2**·dmap·w suitable for X-ray measurement were filtered, washed with ethanol and air-dried. Yield (51 mg, 71%). M.p = 291 °C. Selected IR data (ATR, cm^{-1}): 3166w (OH, water), 2918w (methyl), 1612vs (C=C, C=N), 1589vs (C=C, C=N), 1533s, 1465s, 1381s, 1280s, 1228vs, 1045s, 1016vs, 942vs, 834m, 781vs, 707s, 661vs, 633s. MS (EI, Calc. m/z = 716.72): 606 (M – tolyl – H$_2$O, 100%), 577 (ligand **2** + Co, 20%), 547 (M – 2Me – dmap – H$_2$O, 80%), 121 (dmap, 20%). Anal. calc. for C$_{33}$H$_{33}$CoN$_6$O$_4$S$_2$: C, 55.30; H, 4.64; N, 11.73; S, 8.95%. Found: C, 55.48; H, 4.70; N, 11.47; S, 8.68%.

2.3. *Catalytic oxidation of o-aminophenol to 2-aminophenoxazin-3-one*

Phenoxazinone-synthase-like activity was studied by deploying 100 equivalents of *o*-aminophenol (OAPH) relative to concentration of the individual complexes maintained at 5.0×10^{-5} M in acetonitrile and under aerobic conditions at a thermostat temperature of 25 °C. The reaction was followed spectrophotometrically by monitoring the increase in the absorbance of phenoxazinone chromophore as a function of time at 426 nm (ε = 17,278 M^{-1} cm^{-1}), which is characteristic of 2-aminophenoxazin-3-one in acetonitrile. The 2-aminophenoxazin-3-one molecule was isolated, fully characterized and used for the generation of a calibration curve on the UV–Vis spectrophotometer.

For the catalytic oxidation of 2-amino-4-chlorophenol (Cl-OAPH) to 2-amino-8,10a-dichloro-10,10a-dihydro-3H-phenoxazin-3-one (Cl-APX, Scheme 2), 2.5×10^{-5} M of the complexes was utilized in the presence of 100 equivalents of Cl-OAPH while the increase in absorbance of the phenoxazinone chromophore was monitored at 433 nm. Absorbance spectra of the solutions were measured at time intervals of 30 minutes for all the complexes. The initial rate method was applied to determine the rate of reaction by linear regression from the slope of absorbance values against time.

2.4. *Crystal structure determinations*

Single crystals of the complexes were obtained by slow evaporation of the solution of the complexes in ethanol or methanol. The intensity data for the compounds were collected on a Nonius KappaCCD diffractometer using graphite-monochromated Mo-K$_\alpha$ radiation. Data were corrected for Lorentz and polarization effects; absorption was taken into account on a semi-empirical basis using multiple scans [35–38]. The structures were solved by direct methods (SHELXS) and refined by full-matrix least squares techniques against Fo$_2$ (SHELXL-97 and SHELXL-2014) [38,39]. The hydrogen atoms bonded to the water molecule O5 of **Co2**·dmap·w were located by difference Fourier synthesis and refined isotropically. All other hydrogen atoms were included at calculated positions with fixed thermal parameters. All non-hydrogen and non-disordered atoms were refined anisotropically [38]. The crystal of **Co2**·OAc·bpy contains large voids, filled with disordered solvent molecules. The size of the voids is 281 Å^3/unit cell. Their contribution to the structure factors was secured by back-Fourier transformation using the SQUEEZE routine of the program PLATON [40]. The program *XP* (SIEMENS Analytical X-ray Instruments, Inc. 1994) was used for structure representations [41]. Crystallographic data as well as structure solution and refinement details are summarized in Table 1.

3. Results and discussion

3.1. *Syntheses and characterization of cobalt(III) complexes*

The octahedral cobalt(III) complexes were generally obtained in good yields by allowing Co(OAc)$_2$ and any of ligands **1** or **2** to interact at room temperature in a given solvent and in the presence of a selected co-ligand additive or base. Analytical characterization data of the complexes agree with the expected values and are further confirmed by X-ray crystal structures.

Although the complexes **Co1**·OAc·bpy, **Co2**·OAc·bpy and **Co2**·dmap·w possess mixed-ligand coordination environments, our deployment of triethylamine as a potential co-ligand preferentially yielded only the bis-ligand complex [**Co1$_2$**][Et$_3$NH], where the triethylamine only functions as a base and acts as a counter cation after becoming protonated (Scheme 3(a)). Furthermore, the tendency of these dianionic ligands to oxidize the
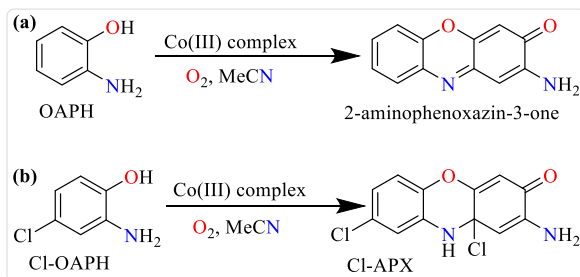
Scheme 2. Aerobic catalytic oxidation of (a) *o*-aminophenol to 2-aminophenoxazin-3-one and (b) 2-amino-4-chlorophenol (Cl-OAPH) to 2-amino-8,10a-dichloro-10,10a-dihydro-3H-phenoxazin-3-one (Cl-APX).
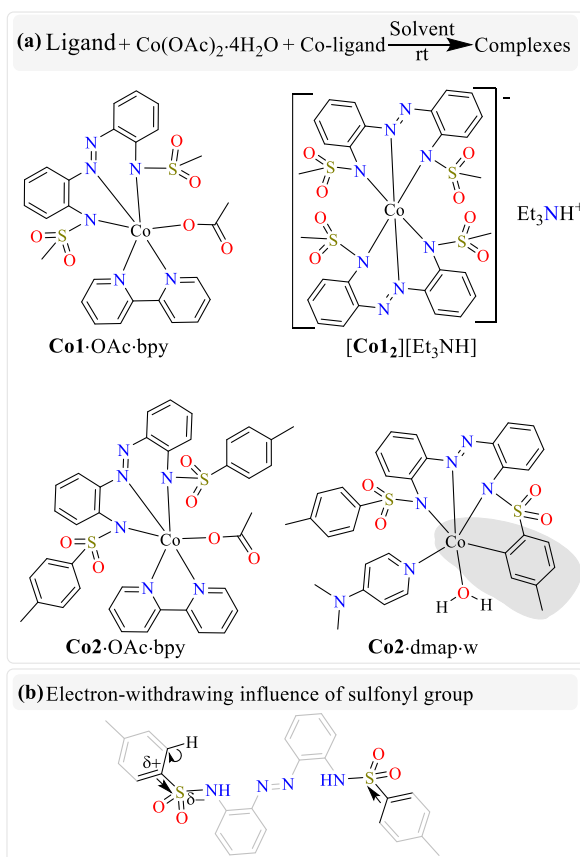
Scheme 3. (a) Synthetic route and compositions of the obtained cobalt(III) complexes. (b) C–H activation of tolyl arm of ligand **2** leading to Co–C cyclometallation.

cobalt(II) starting material into cobalt(III) products is also worthy of note. The very rare organometallic cyclocobaltated bond in **Co2**·dmap·w (shaded regions in Scheme 3(a)), which results from the C–H bond activation of a tolyl ring of ligand **2** (Scheme 3(b)), is also remarkable.

3.2. *X-ray structural analyses*

Complexes **Co1**·OAc·bpy, [**Co1₂**][Et₃NH] and **Co2**·OAc·bpy crystallized in the monoclinic P2₁/n, C2/c and P2₁/c space groups, respectively, while complex **Co2**·dmap·w crystallized in the triclinic

Table 1. Crystal data and refinement details for the X-ray structure determinations

Compound	**Co1**·OAc·bpy	[**Co1₂**][Et₃NH]	**Co2**·OAc·bpy	**Co2**·dmap·w
Formula	$C_{26}H_{25}CoN_6O_6S_2$	$C_{36}H_{52}CoN_9O_{10}S_4$	$C_{40}H_{39}CoN_6O_7S_2$ [*]	$C_{33.5}H_{35}CoN_6O_{5.5}S_2$
fw (g·mol⁻¹)	640.57	958.04	838.82[*]	732.73
°C	−140(2)	−140(2)	−140(2)	−140(2)
Crystal system	monoclinic	monoclinic	monoclinic	triclinic
Space group	P 2₁/n	C 2/c	P 2₁/c	P ī
a/ Å	8.2777(2)	12.7142(2)	10.2788(2)	10.7826(5)
b/ Å	18.0371(5)	20.2034(4)	16.6381(4)	12.1672(6)
c/ Å	18.4623(3)	17.5336(4)	24.9023(5)	14.1688(7)
α/°	90	90	90	74.698(2)
β/°	94.003(1)	107.981(1)	98.559(1)	78.483(2)
γ/°	90	90	90	65.782(3)
V/Å³	2749.80(11)	4283.88(15)	4211.35(16)	1626.32(14)
Z	4	4	4	2
ρ (g·cm⁻³)	1.547	1.485	1.323[*]	1.496
μ (cm⁻¹)	8.29	6.62	5.61[*]	7.1
Measured data	27341	24426	42423	21261
Data with I > 2σ(I)	5610	4493	8547	6554
Unique data (R_{int})	6256/0.0349	4912/0.0313	9615/0.0448	7379/0.0458
wR_2 (all data, on F²)[a)]	0.0767	0.0952	0.2033	0.1112
R_1 ($I > 2\sigma(I)$)[a]	0.0363	0.0376	0.0912	0.0427
S [b]	1.046	1.025	1.235	1.062
Res. dens./e·Å⁻³	0.676/−0.445	0.500/−0.422	0.921/−0.573	0.673/−0.595
Absorpt method	multi-scan	multi-scan	multi-scan	multi-scan
Absorpt corr T_{min}/T_{max}	0.6845/0.7456	0.7001/0.7456	0.6742/0.7456	0.5665/0.7456
CCDC No.	1903078	1903080	1903079	1903081

[*] Derived parameters do not contain the contribution of the disordered solvent.

[a] Definition of the *R* indices: $R_1 = (\Sigma ||F_o| - |F_c||)/\Sigma |F_o|$;

w$R_2 = \{\Sigma[w(F_o^2 - F_c^2)^2]/\Sigma[w(F_o^2)^2]\}^{1/2}$ with $w^{-1} = \sigma^2(F_o^2) + (aP)^2 + bP$; $P = [2F_c^2 + \text{Max}(F_O^2)]/3$;

[b] $s = \{\Sigma[w(F_o^2 - F_c^2)^2]/(N_o - N_p)\}^{1/2}$.

Pī space group (Table 1). Crystal structures revealed that the synthesized ligands formed tridentate five–six-membered N^N^N chelation for complexes **Co1**·OAc·bpy, [**Co1₂**][Et₃NH] and **Co2**·OAc·bpy while tetradentate N^N^N^C chelation is obtained for **Co2**·dmap·w due to cyclocobaltation (Figures 1–4). Such chelations suggest higher coordination stability from ligands **1** and **2** relative to the other coordinated co-ligands. Bond lengths and angles around the coordination centre of the complexes are within the expected values (see **Table S1** of the Supplementary information) [42]. The diversity of coordinative

saturation observed among the obtained complexes fulfils our deliberate aim of studying the influence of diverse coordination environments on catalyst efficiencies.

The interesting C–H activation of an *ortho*-proton on one of the tolyl rings of ligand **2**, which leads to cyclometallation in complex **Co2**·dmap·w, can be attributed to the strong electron-withdrawing influence of the bonded sulfonamide function (Figure 3). A further factor that possibly supports the cyclometallation is the absence of sufficient anionic donors or insufficient pyridyl co-ligands to satisfy the co-
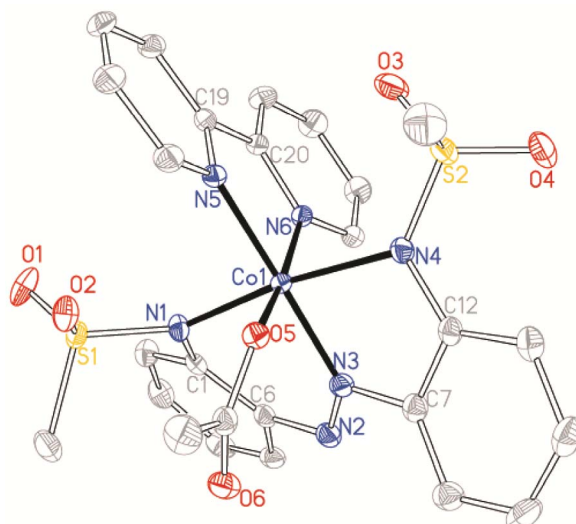
Figure 1. Structure of **Co1**·OAc·bpy with ellipsoids drawn at the 50% probability level. Protons have been omitted for clarity.

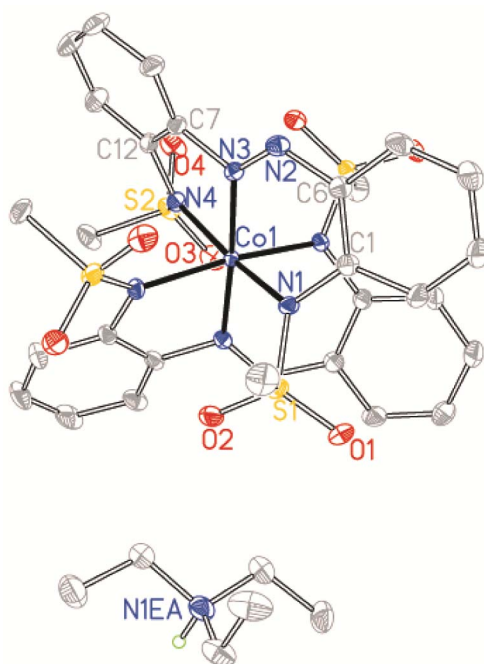**Figure 2.** Structure of [**Co1₂**][Et₃NH] with ellipsoids drawn at the 50% probability level. Protons have been omitted for clarity.

ordinative saturation required by the Co(III) centre. Even a water molecule had to be taken up as the co-ligand to achieve an octahedral geometry. The only few reports of cyclometallated cobalt complexes have been obtained under classical organometallic inert conditions [43–46]. To the best of our knowledge, the formation of a cyclocobaltated complex in the presence of moisture and air as in the preparation of **Co2**·dmap·w is rare. It is therefore plausible to conclude that incorporation of a sulfonamide
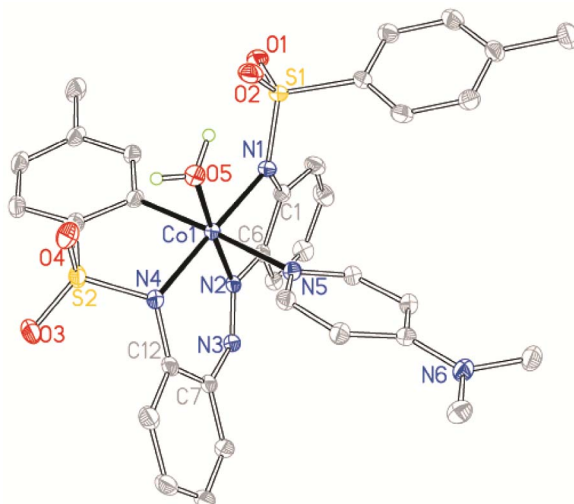
Figure 3. Structure of **Co2**·dmap·w with ellipsoids drawn at the 50% probability level. Protons have been omitted for clarity.
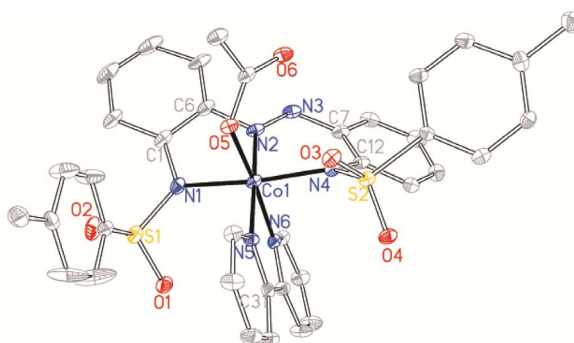
Figure 4. Structure of **Co2**·OAc·bpy with ellipsoids drawn at the 50% probability level. Protons have been omitted for clarity.

substituent could be important for the purpose of facilitating C–H bond activations for organometallic syntheses [47].

In order to properly describe the coordination polyhedra around each cobalt(III) for **Co1**·OAc·bpy, [**Co1₂**][Et₃NH], **Co2**·OAc·bpy and **Co2**·dmap·w, Continuous Shape Measurement (CShM) calculations were carried out by using the experimentally obtained X-ray structural coordinates of the central cobalt atoms and their directly coordinated donor atoms. The results, which are summarized in Table 2, revealed that the coordination polyhedron around each cobalt(III) centre can best be described as octahedral (O_h) [48–50]. The distortion path analysis, which provides the percentage deviation from an

ideal polyhedron on a scale of 0%–100%, revealed the lowest distortions from an ideal octahedron (i.e. 0.348–0.748%) relative to hexagonal pyramid (30.155–32.295%), pentagonal pyramid (25.530–27.265%), trigonal prism (11.964–19.84%) and Johnson pentagonal pyramid (29.178–30.560%) [51]. The complex **Co2**·dmap·w possesses the closest geometry to an octahedron arguably because of the water donor, which allows for the lowest distortive ligand–ligand repulsion and may imply some sort of coordinative stability in **Co2**·damp·w. However, the chelate effect in the bis-ligand complex [**Co1₂**][Et₃NH] would represent a much stronger coordinative stability.

Table 2. Calculated CShM parameters for **Co1**·OAc·bpy, [**Co1₂**][Et₃NH], **Co2**·OAc·bpy and **Co2**·dmap·w

Polyhedron[a]	**Co1**·OAc·bpy	[**Co1₂**][Et₃NH]	**Co2**·OAc·bpy	**Co2**·dmap·w
HP-6 (D_{6h})	32.295	30.155	31.750	31.862
PPY-6 (C_{5v})	25.530	26.011	26.823	27.265
OC-6 (O_h)	0.748[b]	0.673[b]	0.598[b]	0.348[b]
TPR-6 (D_{3h})	11.964	13.963	13.305	14.845
JPPY-6 (C_{5v})	29.178	29.644	30.185	30.560

[a]HP-6 (D_{6h}) = hexagon; PPY-6 (C_{5v}) = pentagonal pyramid; OC-6 (Oh) = octahedron; TPR-6 (D_{3h}) = trigonal prism; JPPY-6 (C_{5v}) = Johnson pentagonal pyramid J2.

[b] Oh has the closest agreement.

Table 3. Catalytic performance of the four complexes in oxidative coupling of OAPH
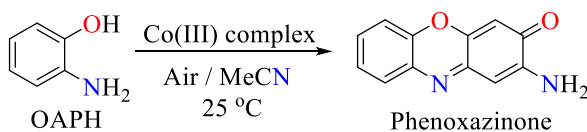
Complex	$10^3 \times V$ (h^{-1})
No complex	0.46
Co1·OAc·bpy	23.30
[**Co1₂**][Et₃NH]	1.15
Co2·OAc·bpy	15.48
Co2·dmap·w	13.30

Reaction conditions: acetonitrile, 1:100 catalyst to OAPH, 25 °C.

3.3. *Phenoxazinone synthase mimicking activity by cobalt complexes*

The phenoxazinone synthase mimicking activity of the complexes was tested via oxidative coupling of OAPH or its derivative 2-amino-4-chlorophenol (Cl-OAPH) in the presence of 1 mol% of cobalt(III) and at 25 °C (Scheme 2). The relative catalytic efficiencies for the various complexes were evaluated via absorbance changes (Figure 5(a and b)) as a function of time. Estimates of the initial rate values (*V*) were determined by linear regression from the slopes of absorbance versus time plots (Figures 6 and 7). These estimates were used for quantitative comparison of catalytic efficiencies among the prepared complexes (Tables 3 and 4).

Insignificant absorbance changes were observed in the absence of the complexes, which proves the importance of the metal ions (Figure 6(a and b) and Table 3). Correlation could be observed between the coordination features and the catalytic outcomes.

The bis-ligand complex [**Co1₂**][Et₃NH], which is the most strongly chelated analogue, has remarkably the least catalytic productivity among the complexes, which could be attributed to the difficulty in releasing the metal centre from the hold of two tridentate chelators. This emphasizes the importance of free coordination sites for the catalysis and that a ligand with strong chelation characteristics as obtainable with porphyrin ligands should be avoided when designing metalloenzyme models.

On the other hand, from a comparison among complexes assembled along with co-ligands [i.e. **Co1**·OAc·bpy (23.30×10^{-3} hr⁻¹) > **Co2**·OAc·bpy (15.48×10^{-3} hr⁻¹) > **Co1**·dmap·w (13.30×10^{-3} hr⁻¹)], the catalyst efficiencies appear to correlate with the percentage extent of deviation from the regular octahedron according to the CShM calculations (i.e. **Co1**·OAc·bpy = 0.748% > **Co2**·OAc·bpy = 0.598% > **Co1**·dmap·w = 0.348%; Table 2). It is therefore plausible to conclude that the general state of steric hindrance in the various coor-
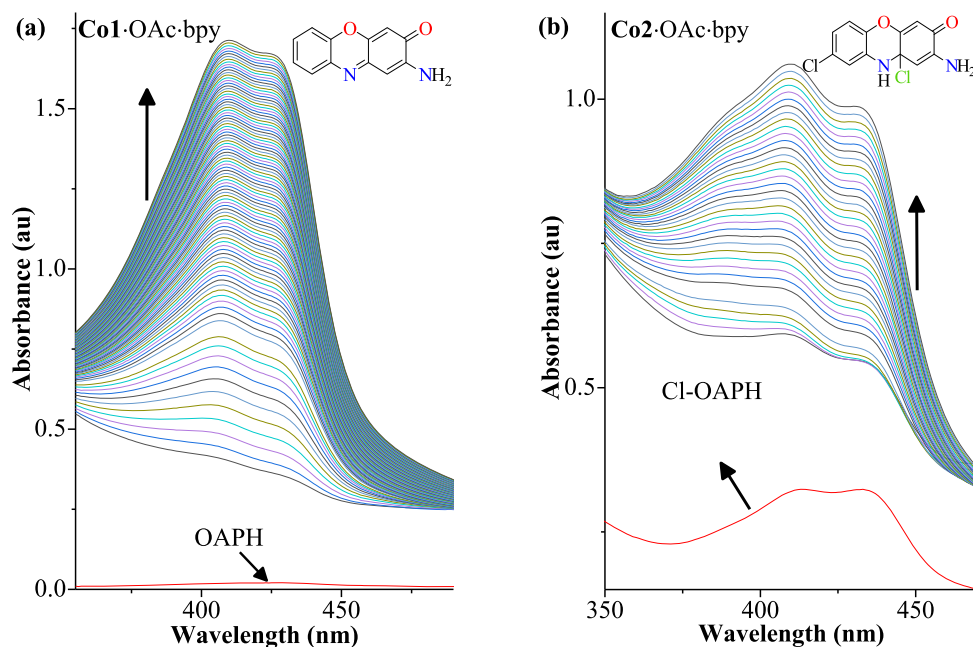
Figure 5. Stack of UV–Vis spectral scans at regular time intervals showing the increasing phenoxazinone chromophore band for substrates in the presence of 1 mol% of cobalt(III) complexes in acetonitrile solution. (a) **Co1**·OAc·bpy + OAPH, 48 hours; (b) **Co2**·OAc·bpy + Cl-OAPH, 12 hours.

dination polyhedra, which is associated with ligand and co-ligand sizes and the corresponding ligand–ligand steric repulsions, may be accountable for the observed differences in catalytic productivities of the different metal centres. A strained coordination polyhedron hints at the readiness for dissociative events, which is required for creating free substrate-binding sites around the metal ion. Additionally, of the three mixed-ligand complexes, the cyclocobaltated complex **Co2**·dmap·w has the tetradentate trianionic complexation feature of ligand **2** as further reason for its poorer catalyst performance.

Complexes **Co1**·OAc·bpy and **Co2**·OAc·bpy, which possess higher catalytic yields for the coupling of OAPH, are further deployed for the coupling of Cl-OAPH at 25 °C. Their resulting initial rates are 32.06×10^{-3} hr^{-1} and 26.06×10^{-3} hr^{-1}, respectively, which reveal higher initial rate values relative to the experiments without cobalt(III) complex (Figure 6(b)). A similar coupling reaction for Cl-OAPH in the absence of cobalt(III) also yielded negligible products (see Supplementary information **Table S2**). Yet it is noteworthy that **Co1**·OAc·bpy shows a higher catalytic efficiency than **Co2**·OAc·bpy towards the

oxidative coupling of Cl-OAPH. It is also worthy of mention that coupling of the chloro-substituted substrate Cl-OAPH is less favoured compared to the non-substituted OAPH, which can be expected on the grounds of steric influence of the chloro-substituent (Figure 6(b) vs. (a)). A proposed scheme of catalytic coupling by complex **Co2**·OAc·bpy has been summarized in Scheme 4.

3.4. *Temperature variation and phenoxazinone mimicking activities*

The effect of temperature variation from 25 °C to 65 °C on the phenoxazinone activity was examined using complexes **Co1**·OAc·bpy, **Co2**·OAc·bpy and **Co2**·dmap·w as catalytic models. The results show a remarkable increase in catalytic activity as the temperature increases (Table 4 and Figure 7). This agrees with the increasing tendency to dissociate co-ligand donors, which then creates vacant coordination sites for substrate binding. Thus, the tendency of the complexes to generate free coordination sites could on one hand depend on the coordinative strain as well as on thermal dissociations on the other hand.
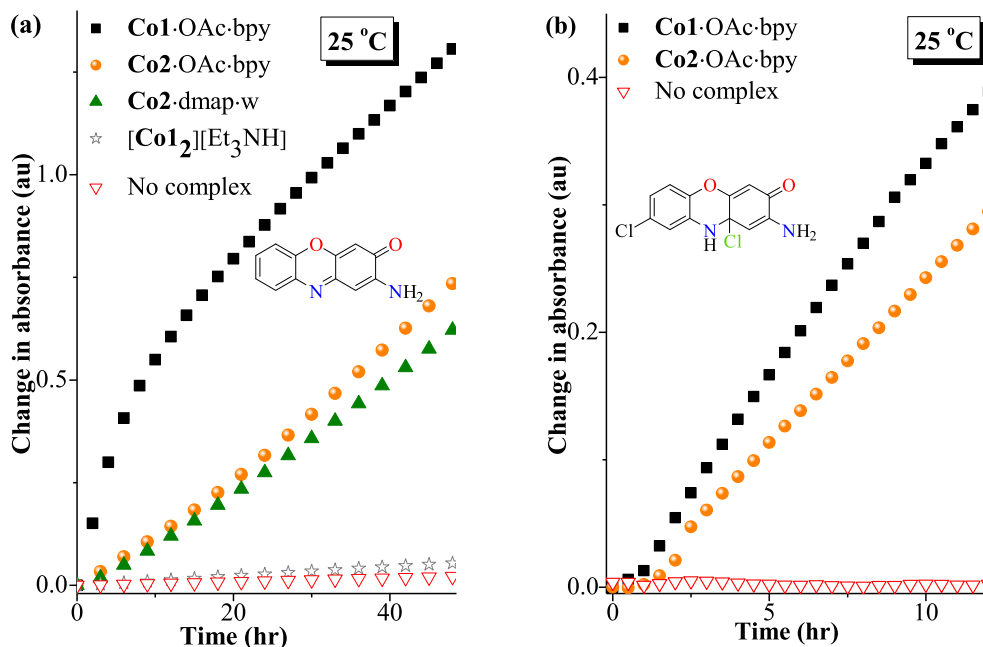
Figure 6. Plot of absorbance *vs* time for the phenoxazinone synthase mimicking activity of complexes at 25 °C. (a) 1 mol% of complex in oxidative coupling of OAPH (5×10^{-3} M). (b) 1 mol% **Co1**·OAc·bpy or **Co2**·OAc·bpy in the catalytic oxidation of Cl-OAPH (2.5×10^{-3} M).
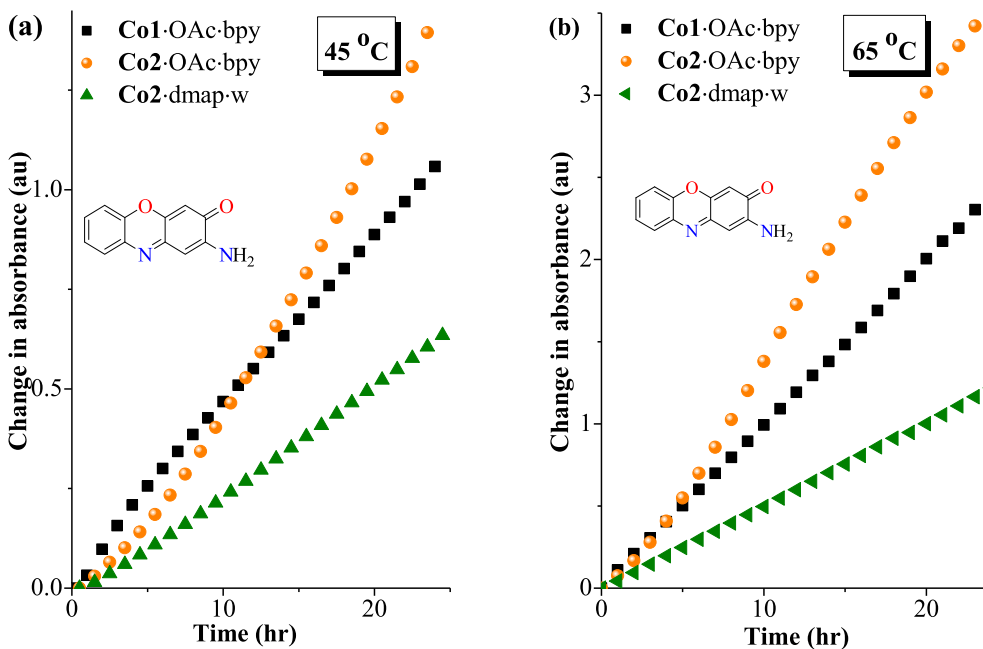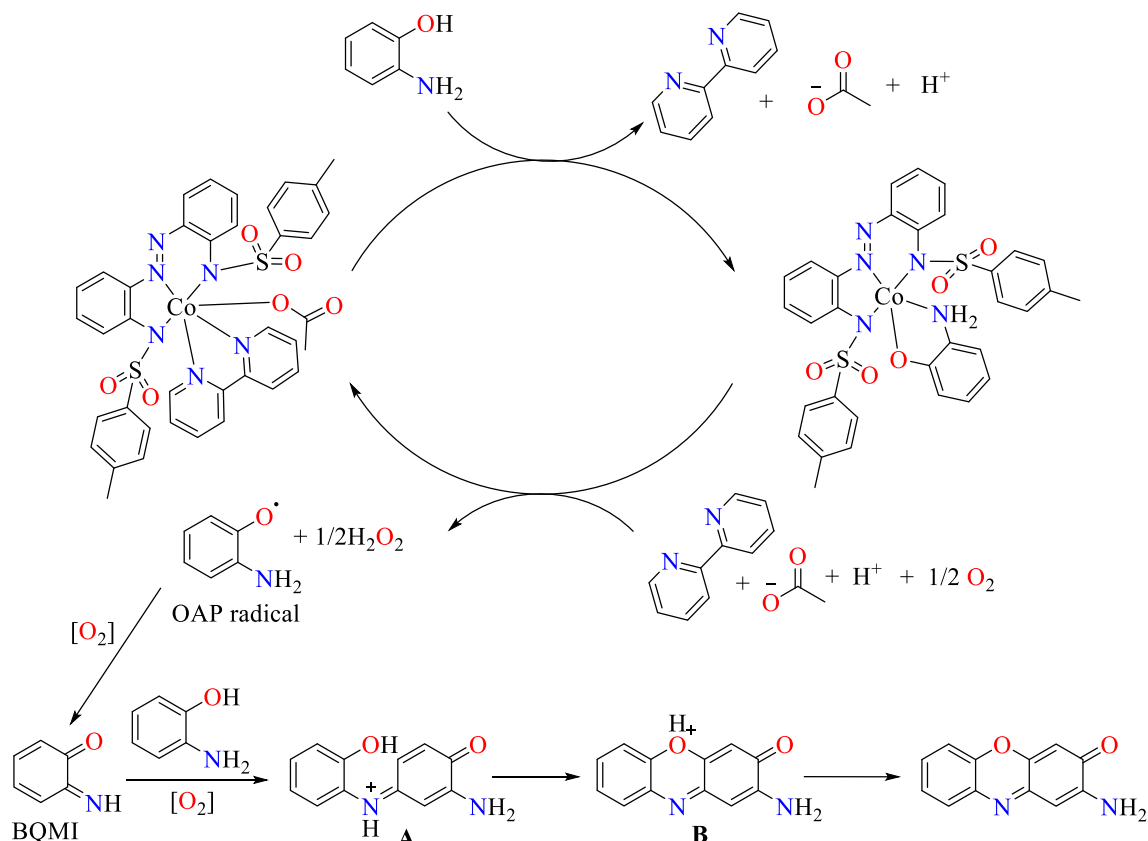

Figure 7. Plot of absorbance *vs* time for the phenoxazinone synthase mimicking activity of complexes at (a) 45 °C and (b) 65 °C (OAPH = 5×10^{-3} M, complex = 5×10^{-5} M).

Scheme 4. Proposed mechanism for the aerobic catalytic oxidation of OAPH to 2-aminophenoxazin-3-one by **Co2**·OAc·bpy.

Table 4. Varying temperatures and corresponding $10^3 \times V$ values for complexes **Co1**·OAc·bpy, **Co2**·OAc·bpy and **Co2**·damp·w

Temp. (°C)	**Co1**·OAc·bpy	**Co2**·OAc·bpy	**Co2**·dmap·w
25	23.30	15.48	13.30
35	27.67	36.91	18.41
45	41.18	63.20	27.14
55	65.89	117.61	37.50
65	99.76	157.87	50.76

Reaction conditions: coupling of OAPH (5×10^{-3} M), 1:100 complex to OAPH, 25–65 °C.

A very important observation during the increase in catalysis temperature from 25 °C (Figure 6(a)) through 35 °C, 45 °C (Figure 7(a)) and 55 °C to 65 °C (Figure 7(b)) is the steady improvement in performance for complex **Co2**·OAc·bpy. This complex displayed the second best efficiency at 25 °C and thereafter overtakes the originally most active complex **Co1**·OAc·bpy from 35 °C (Table 4). The superior activity for **Co2**·OAc·bpy at higher temperatures relative to **Co1**·OAc·bpy might be attributed to a higher susceptibility to the thermal dissociation of acetate or bipyridine co-ligands in **Co2**·OAc·bpy. The bulk-

iness of the tolyl substituents in **Co2**·OAc·bpy appears to be a contributory factor to its thermal susceptibility [52]. In general, the catalysis outcomes suggest that the availability of a vacant binding site during the catalytic process is important.

4. Conclusion

Two well-characterized tridentate NˆNˆN ligands **1** and **2** designed as dianionic disulfonamide–diazo chelators were deployed along with co-ligands such as acetate (OAc), 2,2'-bipyridine (bpy), 4-dimethylaminopyridine (dmap) and/or water (w) to form octahedral cobalt(III) self-assembled complexes from cobalt(II) acetate. These complexes, which were characterized by elemental, spectroscopic and single-crystal structural analyses, were obtained in varying coordination compositions. While **Co1**·OAc·bpy, **Co2**·OAc·bpy and **Co2**·dmap·w were obtained as mixed-ligand complexes, the complex [**Co1$_2$**][Et$_3$NH] assembled as a highly chelated bis-ligand cobaltate(III) anion with a triethylammonium counter cation due to the absence of co-ligands. The sulfonamide group also proved to be useful for enabling C–H bond activation of its substituent aryl rings, which led to cyclocobaltation for the complex **Co2**·dmap·w in the presence of insufficient co-ligands. The tendency of the dianionic ligands **1** and **2** to oxidize cobalt(II) during complexation into cobalt(III) is noteworthy. Continuous Shape Measurement calculations based on the single-crystal geometries of atoms within the coordination spheres of these complexes revealed varying degrees of small deviations from a regular octahedral polyhedron (0.348–0.748%).

Trends of the phenoxazinone synthase mimicking activities by these complexes correlated with their relative tendency to dissociatively create a vacant coordination space for substrate–metal site interactions. While the control catalysis experiment in the absence of the complexes and catalysis in the presence of the highly chelated bis-ligand complex [**Co1$_2$**][Et$_3$NH], respectively, produced negligible and very low coupling efficiencies, the mixed-ligand complexes actively acted as coupling catalysts for the substrates. Furthermore, among the mixed-ligand complexes, correlation is also observed between the extent of octahedron distortion as well as the thermal dissociation potentials and the coupling

activities, which emphasized the importance of generating vacant binding sites for the substrates on octahedral cobalt(III) centres.

A key result drawn from catalytic trends observed among the complexes in this study is that while coordinative steric strain attributable to ligand sizes and their corresponding ligand–ligand repulsions is the determinant at low temperatures, susceptibility to thermal dissociation of co-ligands is the predominant reason for the catalytic behaviour at higher temperatures and is found capable of reversing the low temperature trends.

Supplementary data

Supporting information for this article is available on the journal's website under the article's URL https://doi.org/10.5802/crchim.15 or from the author. It contains the experimental details and randomization protocols.

Crystallographic data (excluding structure factors) have been deposited with the Cambridge Crystallographic Data Centre as supplementary publication CCDC-1903078 for **Co1**·OAc·bpy, CCDC-1903079 for **Co2**·OAc·bpy, CCDC-1903080 for [**Co1$_2$**][Et$_3$NH] and CCDC-1903081 for **Co2**·dmap·w. Copies of the data can be obtained free of charge on application to CCDC, 12 Union Road, Cambridge CB2 1EZ, UK [E-mail: deposit@ccdc.cam.ac.uk].

References

[1] F.-X. Yang, G.-X. Hou, J. Luo, J. Yang, Y. Yan, S.-X. Huang, "New phenoxazinone-related alkaloids from strain Streptomyces sp. KIB-H1318", *J. Antibiot.*, 2018, **71**, 1040-1043.

[2] V. G. Vlasenko, D. A. Garnovskii, G. G. Aleksandrov, N. I. Makarova, S. I. Levchenkov, A. L. Trigub, Y. V. Zubavichus,

A. I. Uraev, Y. V. Koshchienko, A. S. Burlov, "Electrochemical synthesis, structural, spectral studies and DFT calculations of heteroleptic metal-chelates bearing N, N, S tridentate to-sylamino functionalized pyrazole containing Schiff base and 1,10-phenathroline", *Polyhedron*, 2019, **157**, 6-17.

[3] U. Keller, M. Lang, I. Crnovcic, F. Pfennig, F. Schauwecker, "The actinomycin biosynthetic gene cluster of Streptomyces chrysomallus: a genetic hall of mirrors for synthesis of a molecule with mirror symmetry", *J. Bacteriol.*, 2010, **192**, 2583-2595.

[4] C. E. Barry, P. G. Nayar, T. P. Begley, "Phenoxazinone synthase: mechanism for the formation of the phenoxazinone chromophore of actinomycin", *Biochemistry*, 1989, **28**, 6323-6333.

[5] D. I. Ugwu, U. C. Okoro, N. K. Mishra, S. N. Okafor, "Novel Phenoxazinones as potent agonist of PPAR-α: design, synthesis, molecular docking and in vivo studies", *Lipids Health Dis.*, 2018, **17**, 120.

[6] Z. Farhane, F. Bonnier, H. J. Byrne, "An in vitro study of the interaction of the chemotherapeutic drug Actinomycin D with lung cancer cell lines using Raman micro-spectroscopy", *J. Biophoton.*, 2018, **11**, 1-12.

[7] X. Mu, L. Song, Q. Li, R. Yin, X. Zhao, D. Wang, "Comparison of pulsed actinomycin D and 5-day actinomycin D as first-line chemotherapy for low-risk gestational trophoblastic neoplasia", *Int. J. Gynecol. Obstet.*, 2018, **143**, 225-231.

[8] P. B. Gomes, M. Nett, H.-M. Dahse, C. Hertweck, "Pitu-camycin: structural merger of a phenoxazinone with an epoxyquinone antibiotic", *J. Nat. Prod.*, 2010, **73**, 1461-1464.

[9] E. C. Barnes, P. Bezerra-Gomes, M. Nett, C. Hertweck, "Dandamycin and chandrananimycin E, benzoxazines from Streptomyces griseus", *J. Antibiot.*, 2015, **68**, 463-468.

[10] X. Li, W. Shi, Q. Cheng, L. Huang, M. Wei, L. Cheng, Q. Zeng, A. Xu, "Catalytic activation of dioxygen to hydroxyl radical and efficient oxidation of *o*-aminophenol by cobalt(II) ions in bicarbonate aqueous solution", *Appl. Catal. A: General*, 2014, **475**, 297-304.

[11] A. Panja, N. C. Jana, P. Brandão, "Influence of the first and second coordination spheres on the diverse phenoxazinone synthase activity of cobalt complexes derived from a tetradentate Schiff base ligand", *New J. Chem.*, 2017, **41**, 9784-9795.

[12] P. Mahapatra, S. Ghosh, S. Giri, V. Rane, R. Kadam, M. G. B. Drew, A. Ghosh, "Subtle structural changes in (CuIIL)2MnII complexes to induce heterometallic cooperative catalytic oxidase activities on phenolic substrates (H2L = Salen type unsymmetrical schiff base)", *Inorg. Chem.*, 2017, **56**, 5105-5121.

[13] A. Panja, "Syntheses and structural characterizations of cobalt(II) complexes with N4-donor Schiff base ligands: Influence of methyl substitution on structural parameters and on phenoxazinone synthase activity", *Polyhedron*, 2014, **80**, 81-89.

[14] A. D. Schwarz, K. R. Herbert, C. Paniagua, P. Mountford, "Ligand variations in new sulfonamide-supported group 4 ring-opening polymerization catalysts", *Organometallics*, 2010, **29**, 4171-4188.

[15] S. Y. Chow, M. Y. Stevens, L. R. Odell, "Sulfonyl azides as precursors in ligand-free palladium-catalyzed synthesis of sulfonyl carbamates and sulfonyl ureas and synthesis of sulfonamides", *J. Org. Chem.*, 2016, **81**, 2681-2691.

[16] C. Bougheloum, C. Barbey, M. Berredjem, A. Messalhi, N. Dupont, "Synthesis and structural study of N-acetyl-1,2,3,4-tetrahydroisoquinoline-2-sulfonamide obtained using H6P2W18O62 as acidic solid catalyst", *J. Mol. Struct.*, 2013, **1041**, 6-15.

[17] A. Ashraf, W. A. Siddiqui, J. Akbar, G. Mustafa, H. Krautscheid, N. Ullah, B. Mirza, F. Sher, M. Hanif, C. G. Hartinger, "Metal complexes of benzimidazole derived sulfonamide: Synthesis, molecular structures and antimicrobial activity", *Inorg. Chim. Acta*, 2016, **443**, 179-185.

[18] N. U. Hassan Khan, S. Zaib, K. Sultana, I. Khan, B. Mougang-Soume, H. Nadeem, M. Hassan, J. Iqbal, "Metal complexes of tosyl sulfonamides: Design, X-ray structure, biological activities and molecular docking studies", *RSC Adv.*, 2015, **5**, 30125-30132.

[19] M. Mondelli, F. Pavan, P. C. de Souza, C. Q. Leite, J. Ellena, O. R. Nascimento, G. Facchin, M. H. Torre, "Study of a series of cobalt(II) sulfonamide complexes: Synthesis, spectroscopic characterization, and microbiological evaluation against *M. tuberculosis*. Crystal structure of [Co(sulfamethoxazole)$_2$(H$_2$O)$_2$]·H$_2$O", *J. Mol. Struct.*, 2013, **1036**, 180-187.

[20] H.-X. Dai, A. F. Stepan, M. S. Plummer, Y.-H. Zhang, J.-Q. Yu, "Divergent C–H functionalizations directed by sulfonamide pharmacophores: late-stage diversification as a tool for drug discovery", *J. Am. Chem. Soc.*, 2011, **133**, 7222-7228.

[21] M. A. Schmidt, R. W. Stokes, M. L. Davies, F. Roberts, "4-Cyanobenzenesulfonamides: Amine synthesis and protecting strategy to compliment the Nosyl group", *J. Org. Chem.*, 2017, **82**, 4550-4560.

[22] D. Orain, J. Ellard, M. Bradley, "Protecting groups in solid-phase organic synthesis", *J. Comb. Chem.*, 2002, **4**, 1-16.

[23] Y. Sano, A. C. Weitz, J. W. Ziller, M. P. Hendrich, A. S. Borovik, "Unsymmetrical bimetallic complexes with M II–(μ-OH)–M III Cores (M II M III = Fe II Fe III Mn II Fe III Mn II Mn III): Structural, magnetic, and redox properties", *Inorg. Chem.*, 2013, **52**, 10229-10231.

[24] C. Villa-Pérez, I. Oyarzabal, G. A. Echeverría, G. C. Valencia-Uribe, J. M. Seco, D. B. Soria, "Single-ion magnets based on mononuclear cobalt(II) complexes with sulfadiazine", *Eur. J. Inorg. Chem.*, 2016, **2016**, 4835-4841.

[25] U. Hahn, F. Vögtle, G. de Paoli, M. Staffilani, L. de Cola, "Long-lived luminescent dendrimers with a [Ru(dpp) 3] 2+-type core: Synthesis and photophysical properties", *Eur. J. Inorg. Chem.*, 2009, **2009**, 2639-2646.

[26] K. Qian, B. Yan, "Lanthanide/zinc centered photoactive hybrids with functional sulfonamide linkage: Coordination bonding assembly, characterization and photophysical properties", *Polyhedron*, 2010, **29**, 226-231.

[27] M. Li, K. Takada, J. I. Goldsmith, S. Bernhard, "Iridium(III) bis-pyridine-2-sulfonamide complexes as efficient and durable catalysts for homogeneous water oxidation", *Inorg. Chem.*, 2016, **55**, 518-526.

[28] S. Ostovar, P. Prinsen, A. Yepez, H. R. Shaterian, R. Luque, "Catalytic versatility of novel sulfonamide functionalized magnetic composites", *ACS Sustain. Chem. Eng.*, 2018, **6**, 4586-4593.

[29] Y. Song, J. Jiang, J. Ma, Y. Zhou, U. von Gunten, "Enhanced transformation of sulfonamide antibiotics by manganese(IV)

oxide in the presence of model humic constituents", *Water Res.*, 2019, **153**, 200-207.

[30] C. R. Mizdal, S. T. Stefanello, V. da Costa Flores, V. A. Agertt, P. C. Bonez, G. G. Rossi, T. C. da Silva, F. A. Antunes Soares, L. de Lourenço Marques, M. M. A. de Campos, "The antibacterial and anti-biofilm activity of gold-complexed sulfonamides against methicillin-resistant Staphylococcus aureus", *Microb. Pathog.*, 2018, **123**, 440-448.

[31] Z. H. Chohan, H. A. Shad, "Sulfonamide-derived compounds and their transition metal complexes: synthesis, biological evaluation and X-ray structure of 4-bromo-2-[(E)-4-[(3,4-dimethylisoxazol-5 yl)sulfamoyl]phenyl iminiomethyl] phenolate", *J. Appl. Organometal. Chem.*, 2011, **25**, 591-600.

[32] N. U. Hassan Khan, S. Zaib, K. Sultana, I. Khan, B. Mougang-Soume, H. Nadeem, M. Hassan, J. Iqbal, "Metal complexes of tosyl sulfonamides: design, X-ray structure, biological activities and molecular docking studies", *RSC Adv.*, 2015, **5**, 30125-30132.

[33] F. Schwizer, Y. Okamoto, T. Heinisch, Y. Gu, M. M. Pellizzoni, V. Lebrun, R. Reuter, V. Köhler, J. C. Lewis, T. R. Ward, "Artificial metalloenzymes: Reaction scope and optimization strategies", *Chem. Rev.*, 2018, **118**, 142-231.

[34] H. O. Oloyede, J. A. Orighomisan Woods, H. Görls, W. Plass, A. O. Eseola, "N-donor-stabilized Pd(II) species supported by sulphonamide-azo ligands: Ligand architecture, solvent coligands, C–C coupling", *J. Mol. Struct.*, 2020, **1199**, 127030.

[35] COLLECT, Data Collection Software; Nonius B.V., Netherlands, 1998.

[36] Z. Otwinowski, W. Minor, in *Macromolecular Crystallography Part A: Processing of X-Ray Diffraction Data Collected in Oscillation Mode* (C. W. Carter, R. M. Sweet, eds.), Academic Press, 1997.

[37] Bruker-AXS inc., SADABS, Madison, WI, U.S.A., 2002.

[38] G. M. Sheldrick, "A short history of SHELX", *Acta Crystallogr. A*, 2008, **64**, 112-122.

[39] G. M. Sheldrick, "Crystal structure refinement with SHELXL", *Acta Crystallogr. C*, 2015, **71**, 3-8.

[40] A. L. Spek, "PLATON SQUEEZE: a tool for the calculation of the disordered solvent contribution to the calculated structure factors", *Acta Crystallogr. C*, 2015, **71**, 9-18.

[41] Siemens Analytical X-ray Instruments Inc., Siemens 1994. XP: Interactive Molecular Graphics Program, Madison, Winscosin, USA, 1994.

[42] K. Ghosh, S. Roy, A. Ghosh, A. Banerjee, A. Bauzá, A. Frontera, S. Chattopadhyay, "Three mononuclear octahedral cobalt(III) complexes with salicylaldimine Schiff bases: Synthesis, characterization, phenoxazinone synthase mimicking activity and DFT study on supramolecular interactions", *Polyhedron*, 2016, **112**, 6-17.

[43] S. Camadanli, R. Beck, U. Flörke, H.-F. Klein, "First regioselective cyclometalation reactions of cobalt in arylketones: C-H versus C-F activation", *Dalton Trans.*, 2008, 5701-5704.

[44] Y. Boutadla, D. L. Davies, O. Al-Duaij, J. Fawcett, R. C. Jones, K. Singh, "Alkyne insertion into cyclometallated pyrazole and imine complexes of iridium, rhodium and ruthenium; relevance to catalytic formation of carbo- and heterocycles", *Dalton Trans.*, 2010, **39**, 10447-10457.

[45] F. Lu, H. Sun, L. Wang, X. Li, "Preparation of organocobalt complexes through C–F/C–H bond activation of polyfluoroaryl imines", *Inorg. Chem. Commun.*, 2014, **43**, 110-113.

[46] M. R. Meneghetti, M. Grellier, M. Pfeffer, J. Fischer, "Reactivity of cyclocobaltated benzylamine derivatives toward terminal alkynes", *Organometallics*, 2000, **19**, 1935-1939.

[47] D. Tilly, G. Dayaker, P. Bachu, "Cobalt mediated C–H bond functionalization: emerging tools for organic synthesis", *Catal. Sci. Technol.*, 2014, **4**, 2756-2777.

[48] M. Pinsky, D. Avnir, "Continuous symmetry measures. 5. The classical polyhedra", *Inorg. Chem.*, 1998, **37**, 5575-5582.

[49] S. Alvarez, J. Echeverría, "New perspectives on polyhedral molecules and their crystal structures", *J. Phys. Org. Chem.*, 2010, **23**, 1080-1087.

[50] J. Cirera, E. Ruiz, S. Alvarez, "Continuous shape measures as a stereochemical tool in organometallic chemistry", *Organometallics*, 2005, **24**, 1556-1562.

[51] D. Casanova, J. Cirera, M. Llunell, P. Alemany, D. Avnir, S. Alvarez, "Minimal distortion pathways in polyhedral rearrangements", *J. Am. Chem. Soc.*, 2004, **126**, 1755-1763.

[52] H. O. Oloyede, J. A. O. Woods, H. Görls, W. Plass, A. O. Eseola, "Flexible, N-sulfonyl-substituted aliphatic amine ligands in palladium-catalyzed Suzuki–Miyaura C C coupling: Influence of substituents bulkiness and co-ligand size", *Polyhedron*, 2019, **159**, 182-191.